

Title	Group delay engineering using cascaded all pass filters for wideband chirp waveform generation(Main Article (Preprint accepted version))
Author(s)	Bose, Sumanta; Vinoy, K. J.
Citation	Bose, S., & Vinoy, K.J. (2013). Group delay engineering using cascaded all pass filters for wideband chirp waveform generation. 2013 IEEE International Conference on Electronics, Computing and Communication Technologies (CONECCT), pp.1-5.
Date	2013
URL	http://hdl.handle.net/10220/19045
Rights	© 2013 Institute of Electrical and Electronics Engineers (IEEE). This is the author created version of a work that has been peer reviewed and accepted for publication by 2013 IEEE International Conference on Electronics, Computing and Communication Technologies (CONECCT), Institute of Electrical and Electronics Engineers (IEEE). It incorporates referee's comments but changes resulting from the publishing process, such as copyediting, structural formatting, may not be reflected in this document. The published version is available at: [DOI: http://dx.doi.org/10.1109/CONECCT.2013.6469308].

Group Delay Engineering using Cascaded All Pass Filters for Wideband Chirp Waveform Generation

Sumanta Bose

Department of Electronics and Communication Engineering
National Institute of Technology (NIT), Trichy, India
e-mail : sumantabose@gmail.com

K. J. Vinoy

Department of Electrical Communication Engineering
Indian Institute of Science (IISc), Bangalore, India
e-mail : kjvinoy@ece.iisc.ernet.in

Abstract — In this paper a second order all pass filter (APF) is designed and analyzed for its potential application for wideband chirp waveform generation. The group delay of a single stage APF varies with frequency within a narrow band and remains flat elsewhere. Furthermore, it has been found that the component values have a great role in the group delay response of the APF. A two stage cascaded second order APF is adopted to enhance the group delay over a wider band. Genetic algorithm is used to optimize the design parameters of the individual APF stages to obtain a smooth and monotonically increasing group delay response while ensuring good input return loss characteristics. This design approach can be used for generating wideband chirp waveforms that have potential applications in radar, sonar and imaging, delivering improved range resolution.

Keywords - All Pass Filters, Chirp, Delay Equalizers, Genetic Algorithm Optimization, Group Delay

I. INTRODUCTION

Group delay engineering is the study of varying the group delay response of circuits and systems to obtain the desired phase response for the signal envelope [1]. Dispersive circuits/media forms the core of such systems where the group delay T_{gd} is a function of frequency, which results in temporal rearrangement of spectral components [2], thereby generating chirp waveforms [3]. These circuits find applications in spread spectrum communication, radar, sonar, imaging, etc. Chirp waveforms produce short ‘spikes’ in the receiver for targets detected, while monotones produce only an overall ‘envelope’ [4]. The ‘range resolution’ (ΔR) for these cases are:

$$\Delta R_{Monotone} = \frac{v \tau_{out}}{2} \quad (1)$$

$$\Delta R_{Chirp} = \frac{v}{2 \times BW} \quad (2)$$

where v is the velocity of the wave in the medium, τ_{out} is the duration of output waveform and BW is the signal bandwidth. Ideally longer pulses carry greater energy into the medium for better identification of the furthestmost targets. But in case of monotonic ranging, ΔR is directly proportional to τ_{out} , i.e. a high τ_{out} implies a degraded ΔR . This problem is solved with ranging using a wideband chirp waveform where the BW determines ΔR , and a proper choice of BW yields an improved ΔR .

Non-minimum phase filters exhibiting an all-pass response are ideal dispersive structures [1,5] having a flat magnitude response with a smooth and monotonously changing group-

delay profile versus frequency. These are suitable to generate wideband chirp waveforms. In this paper we investigate the design approach for such a filter with wideband characteristics.

II. ALL PASS FILTERS

A. Design

A typical second order lattice APF [6] with pole resonant frequency, ω_r , quality factor, Q and termination impedance, R is shown in figure 1. The design equations of the lumped elements are mentioned alongside.

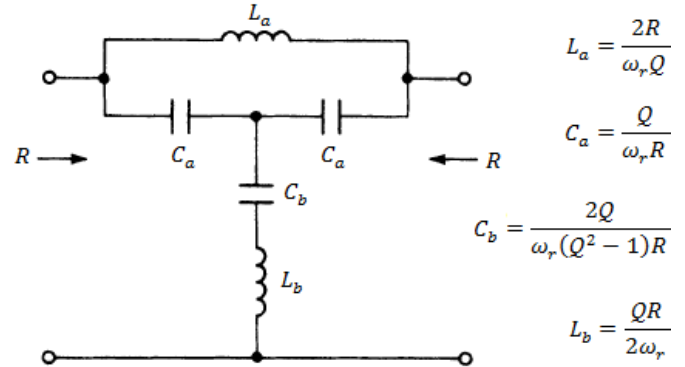


Figure 1. Lumped-element Network of a second order All Pass Filter

The phase shift in radian [6] is :

$$\beta(\omega) = -2 \tan^{-1} \left(\frac{\frac{\omega \omega_r}{Q}}{\omega_r^2 - \omega^2} \right) \quad (3)$$

and the group delay [6] is :

$$T_{gd}(\omega) = \frac{2Q\omega_r(\omega_r^2 + \omega^2)}{Q^2(\omega_r^2 - \omega^2)^2 + \omega^2\omega_r^2} \quad (4)$$

The frequency of maximum delay $\lesssim \omega_r$, is expressed as [6] :

$$\omega(T_{gd,max}) = \omega_r \sqrt{4 - \frac{1}{Q^2} - 1} \quad (5)$$

For practical purposes, ω_r , Q and $T_{gd,max}$ are related [6] as :

$$T_{gd,max} = \frac{4Q}{\omega_r} \quad (6)$$

It has three design parameters, viz. ω_r , Q and $T_{gd,max}$ of which any two may be independently chosen by the designer. As we see in figure 2, by fixing f_r at 1.3445GHz and varying

Q , we get correspondingly different $T_{gd,max}$; and vice-versa, by varying $T_{gd,max}$ we get correspondingly different Q .

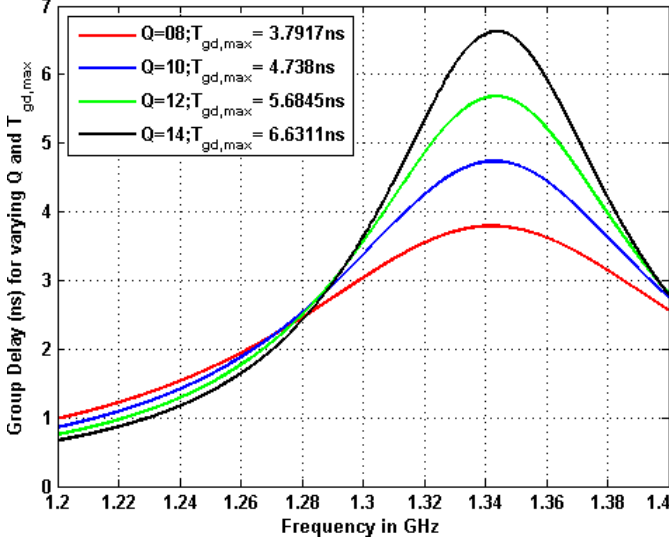


Figure 2. Comparison of group delay curves for different Q and $T_{gd,max}$

Note that fixing the ω_r and $T_{gd,max}$ determines the Q uniquely as shown in figure 3, where the plot in black has a $f_r = 1.3445\text{GHz}$ and $T_{gd,max} = 6.6311\text{ns}$ determining $Q = 14$. However we may adopt a graphical approach wherein the group delay curve is made to pass through $(m \cdot \omega_r, n \cdot T_{gd,max})$ where $0 < \{m, n\} < 1$; as exemplified in figure 3, by the plots in green, red and blue. Enforcing such a condition on the APF design affects its quality factor, Q , derived as :

$$Q = \sqrt{\frac{(m^2 + 1) - 2m^2n}{2n \cdot (m - 1)^2}} \quad (7)$$

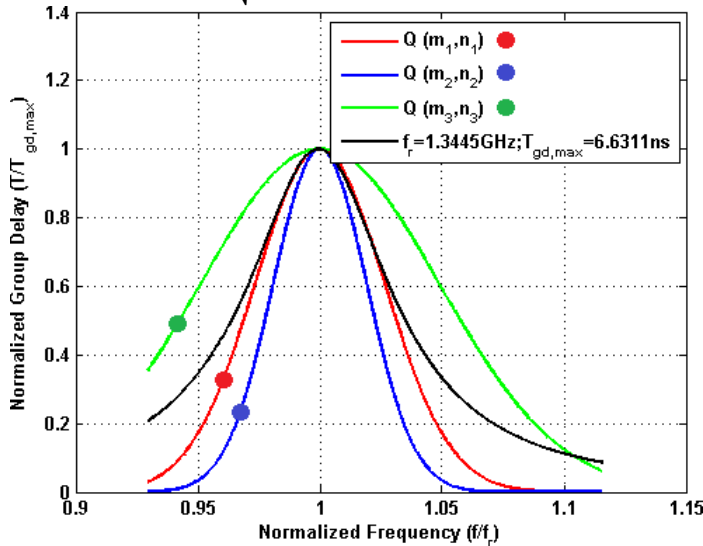


Figure 3. Graphical approach to engineer group delay curve affecting Q

For a near-perfect match and respectable return loss characteristics, m and n must be chosen such that Q obtained is not less than 8 ($Q \nless 8$). For $Q < 8$, the APF's circuit element attain practically unrealizable values, as is evident

from the design equations.

B. Sensitivity Analysis of Various Lumped Elements

Co-solving the element design equations with equations 3, 4 and 5 yields ω_r , Q , $\beta(\omega)$ and T_{gd} as functions of the individual lumped elements, as :

$$\omega_r = \sqrt{\frac{2}{L_a C_a}} \quad (8)$$

$$Q = \sqrt{\frac{2L_b C_b}{2L_b C_b - L_a C_a}} \quad (9)$$

$$\beta(\omega) = -2 \tan^{-1} \left(\frac{\omega \sqrt{(L_a C_a) \cdot (2L_b C_b - L_a C_a)}}{(2 - \omega^2 L_a C_a) \sqrt{L_b C_b}} \right) \quad (10)$$

$$T_{gd}(\omega) = \frac{2 \cdot \sqrt{\frac{4L_b C_b}{(L_a C_a) \cdot (2L_b C_b - L_a C_a)}} \cdot \left(\omega^2 + \frac{2}{L_a C_a} \right)}{\left(\frac{2L_b C_b}{(2L_b C_b - L_a C_a)} \right) \cdot \left(\omega^2 - \frac{2}{L_a C_a} \right)^2 + \frac{2\omega^2}{L_a C_a}} \quad (11)$$

Equation (8 – 11) gives us a direct insight on the effect of each element on the APF's f_r and its performance; and is used for sensitivity analysis of individual element.

In the present work, the group delay, T_{gd} of the second order APF network is of interest. Each circuit element is tested for their individual sensitivities towards T_{gd} . It is computed at a constant f_r by examining the differential change in T_{gd} (equation 11) due to a differential change in the lumped element value (figure 1) while keeping all others constant. The significance of this is T_{gd} prediction in case of deviation of elements from ideal values during circuit realization.

In a set of MATLAB experiments, we take a sample case, where, $f_r = 1.3445\text{GHz}$ and $Q = 12.2549$. The T_{gd} is observed as a 3D sensitivity plot, as shown in figures 4 to 7.

All the four cases are studied within a frequency range of $\pm 50\text{MHz}$ i.e. approximately $\pm 3.73\%$ around f_r . Thereafter, the sensitivity of each element about their ideal values (denoted by ρ) are tabulated in Table 1.

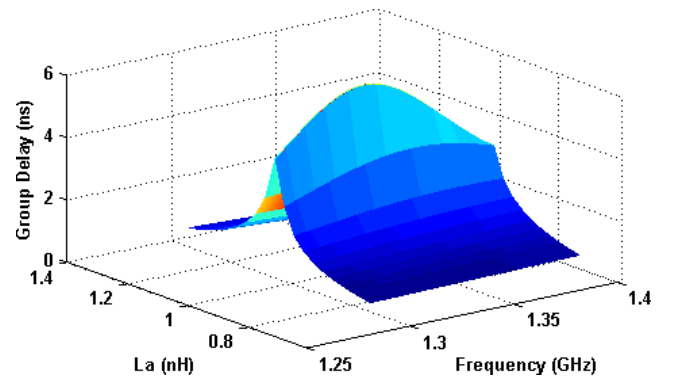


Figure 4. Sensitivity Plot of L_a

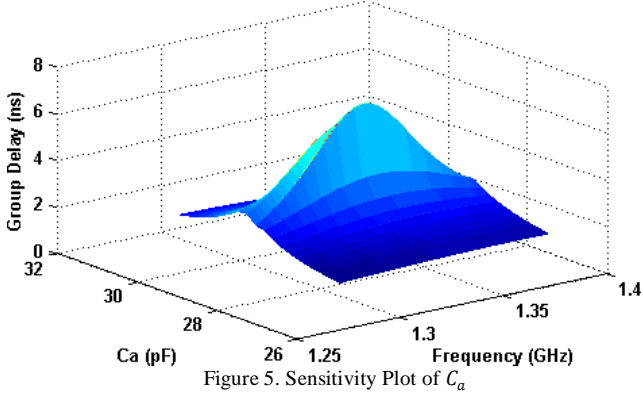


Figure 5. Sensitivity Plot of C_a

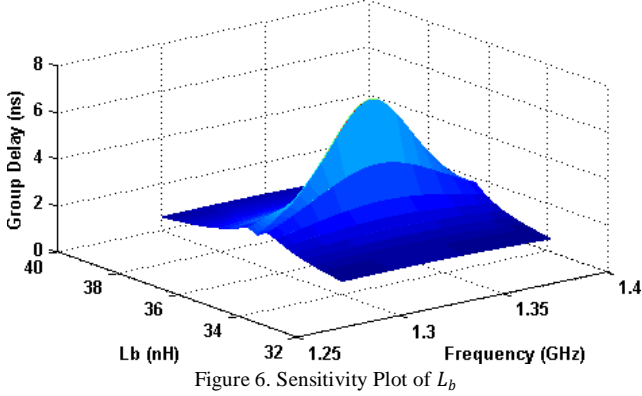


Figure 6. Sensitivity Plot of L_b

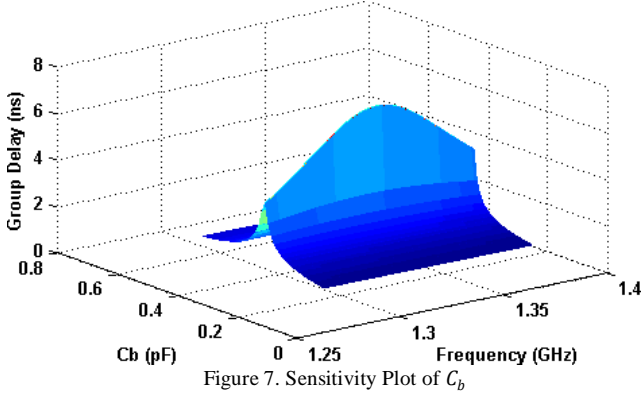


Figure 7. Sensitivity Plot of C_b

TABLE 1. ELEMENT, IDEAL VALUE AND SENSITIVITY IN THE SINGLE STAGE APF PROTOTYPE (FIGURE 1)

Element	Ideal Value	Sensitivity, ρ
L_a	0.965 nH	∓ 447 ns/nH
C_a	29.013 pF	∓ 15 ns/pF
L_b	36.266 nH	∓ 12 ns/nH
C_b	0.383 pF	∓ 1153 ns/pF

We identify that $\rho_{L_b} < \rho_{C_a} < \rho_{L_a} < \rho_{C_b}$. Special care must be taken during fabrication of highly sensitive elements, such as L_a and C_b . If the distributed element values exceeds acceptable limits, it would be good to replace them with more accurate lumped elements. Surface mount multilayer ceramic chip capacitors are known to be reliable, with manufactured

accuracies as high as 99% [7]. Surface mount thin film chip inductors are also quite reliable, with manufactured accuracies as high as 97% [8]. However, in case of unrealizable or extremely sensitive element values, suitable transformations can be performed in order to obtain a realizable APF network, with negligible compromise on the system response [9].

III. CASCADED ALL PASS FILTER NETWORKS

The single stage APF discussed in the previous section provides only a limited bandwidth and is often insufficient to generate waveforms of desired bandwidth. In order to enhance bandwidth, it is possible to design multi-stage all pass filters, each designed with specific resonant frequency and delay response. In cascaded APFs, the magnitude response remains nearly the same, while the time delay gets added algebraically. However, the return loss of the combination differs from the individual APF networks.

The bandwidth does not improve if one were to design these stages at the same resonant frequency. Therefore, in a set of MATLAB simulations, the $T_{gd,net}$ and net return loss of a two stage cascaded second order APF were studied for three cases, as shown in figure 8 and 9. The f_r of the 1st stage was kept constant at $f_{r1} = 1.3$ GHz. The $T_{gd,max}$ of the 1st and 2nd stage were fixed at $T_{gd,max1} = 3.5$ ns and $T_{gd,max2} = 3$ ns respectively. For the 2nd stage, f_{r2} was varied as $f_{r2} = 1.1$ GHz (green plot); $f_{r2} = 1.15$ GHz (blue plot) and $f_{r2} = 1.2$ GHz (red plot) as shown in the group delay response in figure 8. The corresponding net return loss characteristics is shown in figure 9, maintaining the plot color convention. Note that it is important to maintain a respectable net return loss to ensure maximum power transmission. Practically, a maximum tolerable net return loss limit could be -10 dB.

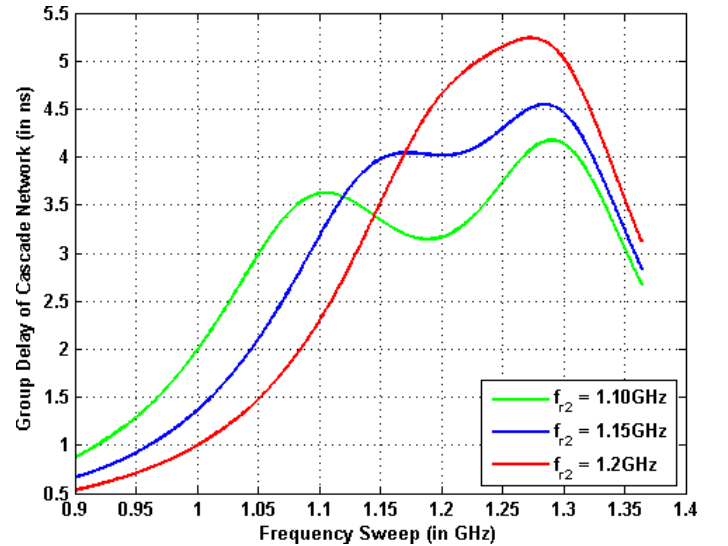


Figure 8. Comparison of group delay for different cascaded APFs

Moreover, the design parameters of these independent APF stages must be such chosen that we get a smooth and monotonic $T_{gd,net}$ curve over the entire frequency range.

This would ensure that different frequency components are delayed differently, thereby giving a spread of various frequency components in time domain, to generate the wideband chirped waveform. However for this, the intermediate dips as shown in the green and blue plots in figure 8 must be avoided.

Therefore, to optimize the two stage cascaded second order APF performance over a wideband, we adopt Genetic Algorithm (GA) [10] to optimize the design parameters of the individual APF stages. The criterion of optimization is that the maximum tolerable net return loss is -10dB over the entire frequency range, and the group delay response is monotonically increasing, exhibiting wideband characteristics. The GA optimization is run by iteratively varying f_r and $T_{gd,max}$ of the individual sections within the ranges tabulated in Table 2. After a number of generations (iterations), their population swarm converges appreciably and we obtain their optimum values as tabulated in Table 2.

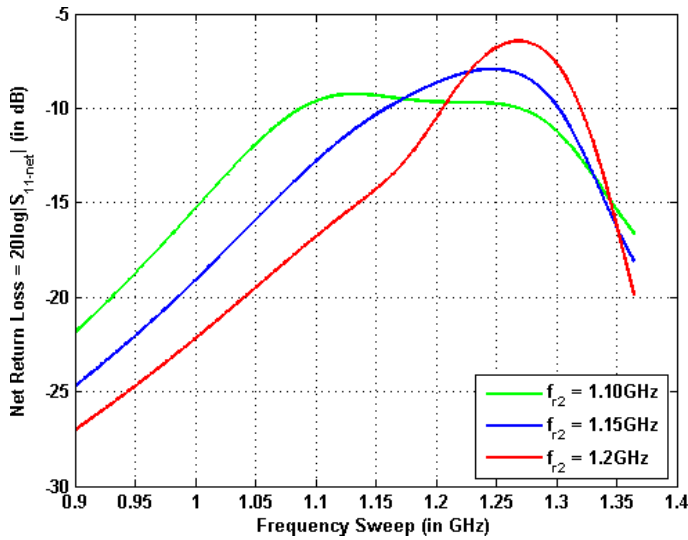


Figure 9. Comparison of net return loss for different cascaded APFs

TABLE 2. PARAMETER, RANGE AND OPTIMUM VALUES USING GENETIC ALGORITHM OPTIMIZATION

Parameter	Range	Optimum Value
f_{r1}	1 GHz to 1.2 GHz	1.085 GHz
$T_{gd,max1}$	3 ns to 5 ns	3.5660 ns
f_{r2}	1.1 GHz to 1.3 GHz	1.2100 GHz
$T_{gd,max2}$	5 ns to 7 ns	5.7600 ns

The two stage cascaded second order APF is constructed with the optimized values tabulated in Table 2 and its group delay response is plotted within our interested frequency range, $f \in [0.9, 1.2]$ GHz in figure 10, which shows its wideband monotonic behavior. Moreover, the net return loss in this range is better than -10dB for all frequencies, as plotted in figure 11. This significantly satisfies both the optimization criterions of GA and we are able to design an overall system (characterized by figure 10 and 11) capable of generating a wideband chirp waveform.

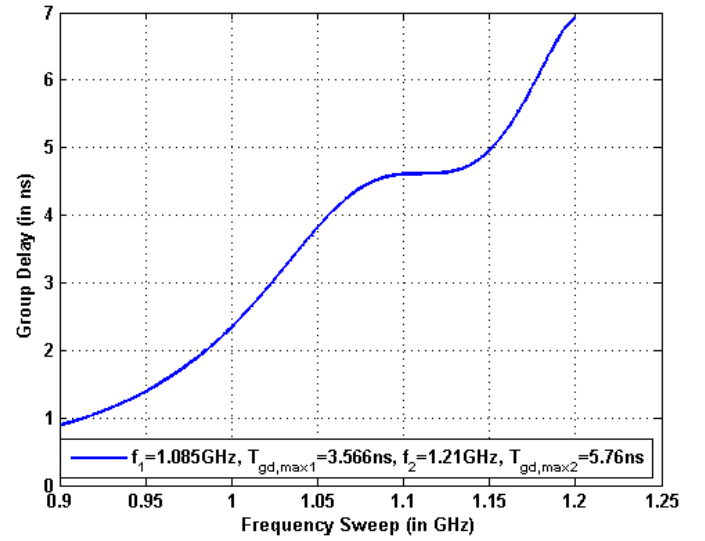


Figure 10. Realized group delay responses of optimized cascaded 2 stage APF network

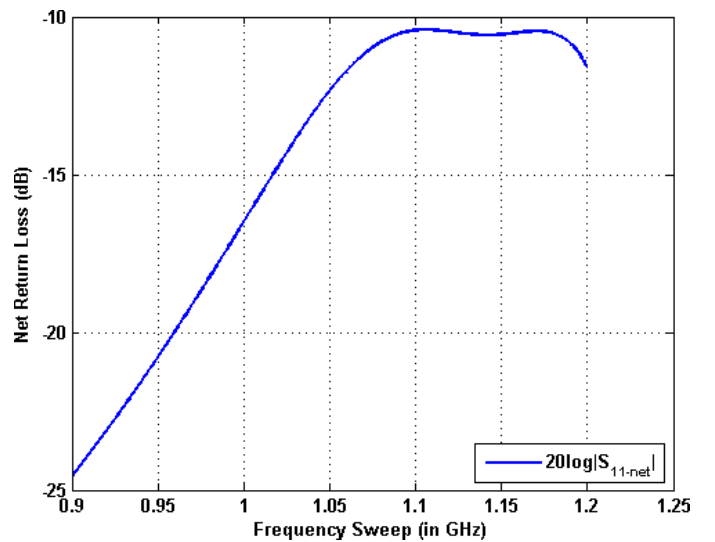


Figure 11. Realized Net Return Loss of optimized cascaded 2 stage APF network

IV. RESULTS FOR WAVEFORM GENERATION

The circuit for wideband chirped waveform generation using a two stage cascaded APF can be characterized by passing summed signals of different frequencies through it. The individual signals undergo different temporal shifting depending on the net delay at the frequency. Consider for example a case as shown through figure 12 to 14, where the input signal (red plot) is of 6 ns window duration, constructed by summing two signals of frequency: 0.9 GHz and 1.2 GHz. A two stage cascaded second order APF modeled using the optimized values from Table 2, gives an output as shown by the blue plot in figure 12. However, we estimate the expected output signal by artificially shifting the individual input signals by an amount of phase found from the phase of the net S_{21} curve. We find from the phase of the net S_{21} curve that the 0.9 GHz signal undergoes a phase shift of -64.5557° while the 1.2 GHz signal undergoes a phase shift of -425.277° . This

expected output is shown by the green plot in figure 12.

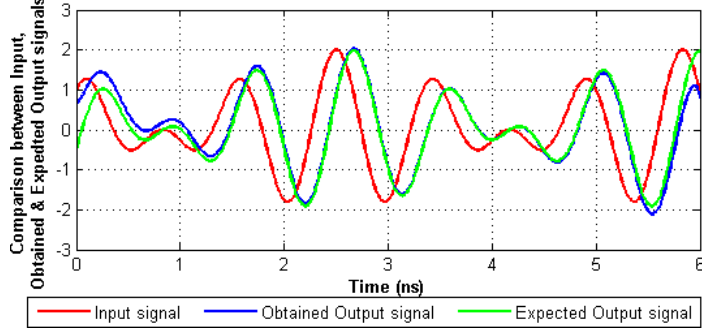


Figure 12. Comparison of input, obtained and expected output signals

The results are satisfactory in the entire window duration, except at the ends where there is a non-overlap of the obtained and expected output. This arises due to slight impedance mismatch as indicated by the net return loss curve in figure 11.

The frequency spectrum of the input, obtained output and expected output signals are generally similar, with slight variations near the constituent signal frequencies, i.e. 0.9 GHz and 1.2 GHz. A detailed comparison of the frequency spectrums of these three signals near 0.9 GHz and 1.2 GHz demonstrates these slight variations, as shown in figure 13 and 14 respectively (maintaining the plot color convention).

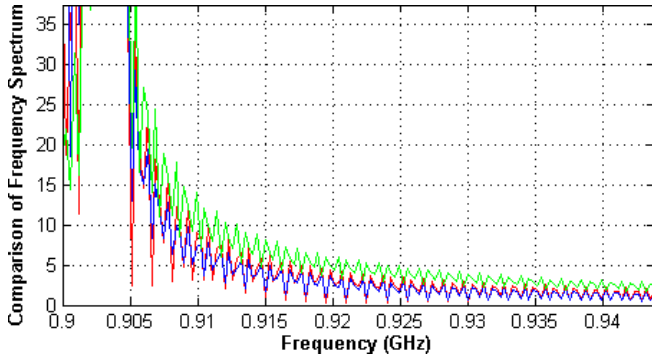


Figure 13. Comparison of frequency spectrum near 0.9 GHz

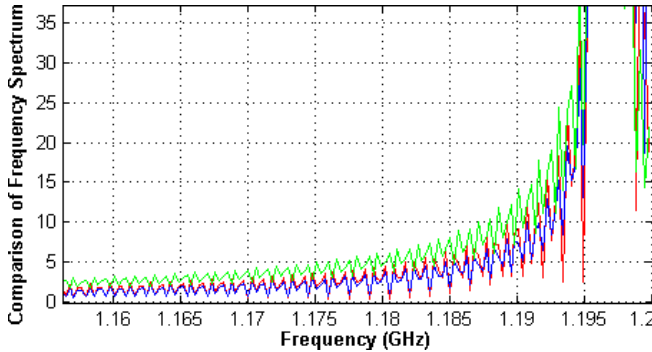


Figure 14. Comparison of frequency spectrum near 1.2 GHz

These results indicate that the two constituent frequency components are delayed differently by the circuit, which results in a change in the time-domain waveform.

Therefore, it is postulated that if one could pass through this filter, multiple frequency components, all starting at the same time instant, a chirped waveform would result.

V. SUMMARY

In this paper we have laid out an approach to design a two stage cascaded second order APF, capable of generating wideband chirp waveforms. Genetic Algorithm based optimization can easily extend the design to multiple stages of the filter to get wider bandwidth. The group delay response of single stage APF is appreciable only for a very narrow range of frequency. It is also quantitatively shown that the response is varying sensitive to individual element values.

Furthermore, temporal shifting of different frequency components is also demonstrated as they pass through the filter. The approach demonstrated here is generally scalable as the design parameters of the individual all pass filter stages can be chosen according to the requirement. This circuit can therefore be used to generate wideband chirped waveforms for radar, sonar and imaging applications, delivering improved range resolution.

REFERENCES

- [1] S. Gupta, C. Caloz, *et al.*, "Group-delay engineered noncommensurate transmission line all-pass network for analog signal processing", *IEEE Transactions on Microwave Theory & Techniques*, Vol. 58, Issue. 9, pp. 2392-2407, Sept. 2010.
- [2] G. P. Agarwal, *Nonlinear Fiber Optics*, Elsevier Publications, New York, 2005.
- [3] "Chirp", *Wikipedia, The Free Encyclopedia*. [Online]. Available: <http://en.wikipedia.org/wiki/Chirp>
- [4] J. E. Ehrenberg, T. C. Torkelson, "FM slide (chirp) signals: a technique for significantly improving the signal to noise performance in hydroacoustic assesment systems", *Elsevier Fisheries Research*, 47, pp. 193-199, 2000.
- [5] G. L. Matthaei, L. Young, E. M. T. Jones, *Microwave Filters, Impedance Matching Networks and Coupling Structures*, McGraw-Hill, New York, 1965.
- [6] A. B. Williams, F. J. Taylor, *Electronic Filter Design Handbook*, McGraw-Hill Professional Publishing, 2006.
- [7] Vishay, *Capacitors - Multilayer SMD*. [Online]. Available: <http://www.vishay.com/capacitors/ceramic-multilayer-smd/>
- [8] Vishay, *Inductors - Surface mount*. [Online]. Available: <http://www.vishay.com/inductors/surface-mount/>
- [9] R. Levy, "Realization of practical lumped element all-pass networks for delay equalization of RF and microwave filters", *IEEE Transactions on Microwave Theory & Techniques*, Vol. 59, Issue. 12, pp.3307-3311, Dec 2011.
- [10] F. Mahmud, S. T. Zuhori, *Genetic Algorithm*, Lap Lambert Academic Publishing, 2012